HHS Public Access

Author manuscript

Neuroscience. Author manuscript; available in PMC 2017 May 03.

Published in final edited form as:

Neuroscience. 2016 May 3; 321: 197–209. doi:10.1016/j.neuroscience.2015.07.041.

Bidirectional modulation of anxiety-related and social behaviors by amygdala projections to the medial prefrontal cortex

Ada C. Felix-Ortiz[1], **Anthony Burgos-Robles**[1], **Neha D. Bhagat**[1,2], **Christopher A. Leppla**[1], and **Kay M. Tye**[1]

Ada C. Felix-Ortiz: acfo@mit.edu; Anthony Burgos-Robles: aburgos@mit.edu; Neha D. Bhagat: bhagat.n@husky.neu.edu; Christopher A. Leppla: cleppla@mit.edu; Kay M. Tye: kaytye@mit.edu

[1]Picower Institute for Learning and Memory, Department of Brain and Cognitive Sciences, Massachusetts Institute of Technology, Cambridge, Massachusetts, USA 02139

[2]Program in Behavioral Neuroscience, Northeastern University, Boston, Massachusetts, USA 02115

Abstract

The basolateral amygdala (BLA) and the medial prefrontal cortex (mPFC) modulate anxiety and social behaviors. It remains to be elucidated, however, whether direct projections from the BLA to the mPFC play a functional role in these behaviors. We used optogenetic approaches in behaving mice to either activate or inhibit BLA inputs to the mPFC during behavioral assays that assess anxiety-like behavior and social interaction. Channelrhodopsin-2 (ChR2)-mediated activation of BLA inputs to the mPFC produced anxiogenic effects in the elevated-plus maze and open-field test, whereas halorhodopsin (NpHR)-mediated inhibition produced anxiolytic effects. Furthermore, activation of the BLA-mPFC pathway reduced social interaction in the resident-intruder test, whereas inhibition facilitated social interaction. These results establish a causal relationship between activity in the BLA-mPFC pathway and the bidirectional modulation of anxiety and social behaviors.

Keywords

optogenetics; amygdala; prefrontal; prelimbic; infralimbic; fear; stress; anxiety disorders; social

1.0 Introduction

The basolateral amygdala complex (BLA) is considered to be a crucial neural hub for the modulation of anxiety-related and emotionally-driven behaviors (Bremner 2004; Dias et al.

Corresponding author: Kay M. Tye, PhD, Picower Institute for Learning and Memory, Dept. of Brain and Cognitive Sciences, Massachusetts Institute of Technology, 77 Massachusetts Ave, Bldg 46-6263, Cambridge, MA 02139, kaytye@mit.edu.

Author Contributions

ACFO and KMT designed experiments. ACFO and CAL performed surgeries. ACFO and NDB performed experiments. ACFO, ABR, and NDB performed histological verification. ABR, ACFO, and KMT wrote the manuscript.

2013; Davis 1992; Tye et al. 2011; Felix-Ortiz et al. 2013; Janak and Tye 2015; Namburi et al. 2015; Allsop et al. 2014). In humans, the BLA exhibits hyperactivity in most forms of anxiety disorders (Rauch, Shin, and Wright 2003), and in rodents BLA hyperexcitability and hypertrophy is associated with an enduring facilitation of anxiety-like behaviors (Roozendaal, McEwen, and Chattarji 2009; Rosenkranz, Venheim, and Padival 2010). Along with a critical role in anxiety, research has established a crucial role of the BLA in the modulation of social behavior (Kling and Steklis 1976; Katayama et al. 2009; Bickart, Dickerson, and Feldman Barrett 2014; Felix-Ortiz and Tye 2014). Given the common comorbidity between anxiety disorders and social deficits (Stein and Stein 2008; Kennedy and Adolphs 2012; American Psychiatric Association 2013), increasing efforts have been directed to understand the BLA mechanisms underlying the regulation of anxiety and social behaviors (Allsop et al. 2014).

Despite substantial existing research examining the role of the BLA in anxiety-related and social behaviors, there is still much work to do in elucidating how the BLA interacts with downstream structures to modulate these behaviors. Application of optogenetics to manipulate specific projections (Boyden et al. 2005; Tye and Deisseroth 2012; Deisseroth 2011; Tye et al. 2011) allows us to map the functional role of discrete neural projections with high cellular and temporal precision. We have already tested the functional role of some BLA targets, such as the central nucleus of the amygdala (CeA) and the ventral hippocampus (vHPC), and found that optogenetically-mediated activation or inhibition of neural transmission from the BLA to either region produces bidirectional changes in anxiety-like behavior (Tye et al. 2011; Felix-Ortiz et al. 2013). In addition, we have observed bidirectional modulation of social behavior by targeting the BLA-vHPC pathway (Felix-Ortiz and Tye 2014). These findings support the hypothesis that BLA interactions with downstream targets such as the CeA and vHPC are sufficient to alter anxiety, and that distinct projections can contribute opposing forces in guiding anxiety-related behavior.

Recent attention has been given to the medial prefrontal cortex (mPFC), which shares reciprocal projections with the BLA (Hoover and Vertes 2007; Pitkänen 2000; Gabbott et al. 2005), and exhibits profound alterations in a wide range of anxiety and social disorders (Milad and Rauch 2007; Gotts et al. 2012). Electrophysiological recordings have revealed that increased excitability in the mPFC correlates with heightened anxiety-related behavior in the open-field test and elevated-plus maze (Bi et al. 2013), and that some populations of mPFC neurons fire preferentially to the “anxiogenic” open arms of the plus maze versus the “safe” closed arms, and vice versa (Adhikari, Topiwala, and Gordon 2011). The mPFC, along with the BLA (Likhtik et al. 2014; Likhtik and Paz 2015), is capable of representing states of high and low anxiety. The mPFC has also been shown to represent social interactions, with some populations of neurons exhibiting increased activity and others showing decreased activity during bouts of social interaction (Jodo et al. 2010). Thus, the mPFC appears to be a key component of the neural circuitry underlying social and anxiety-related behaviors. Although it has been proposed that direct interactions between the BLA and mPFC may be vital for the modulation of anxiety and social behaviors (McClure et al. 2007; Adhikari 2014), a causal role for BLA projections to the mPFC have yet to be established for social and anxiety-related behaviors. Using projection-specific optogenetic

approaches in freely-moving mice, we tested how activation or inhibition of BLA projections to the mPFC modulates anxiety-like and social behaviors.

2.0 Experimental Procedures

2.1 Subjects

All procedures were approved by the Massachusetts Institute of Technology Committee on Animal Care, in accordance with the NIH Guide for the Care and Use of Laboratory Animals. All experiments were conducted on wild-type male C57BL/6 mice aged 6–7 weeks (Jackson Laboratory, Bar Harbor, ME). A total of 43 mice were used in this study. Mice were group-housed in clear Plexiglas homecages with access to food and water *ad libitum*. Mice were maintained on a 12-hr reverse light/dark cycle. For social interaction experiments, 3–4 week-old juvenile male C57BL/6 mice were used as the social stimuli (intruders).

2.2 Surgery

Mice were anesthetized with 1.5–2.0% isoflurane gas/oxygen mixture and mounted on a stereotaxic apparatus (Kopf Instruments, Tujunga, CA) for viral transduction of the BLA. A midline incision was made down the scalp and craniotomies were made using a dental drill. The stereotaxic coordinates used for BLA transfection were −1.16 mm anterior-posterior (AP), ±3.35 mm medial-lateral (ML), and −4.9 mm dorsal-ventral (DV), relative to bregma. A 10-μl microsyringe with a 33-Ga needle (Nanofil; WPI, Sarasota, FL) was used to deliver the viral solutions into the BLA at a rate of 0.1 μl/min using a microsyringe pump (UMP3/Micro4; WPI, Sarasota, FL).

For inhibition, bilateral viral transduction of the BLA (0.5 μl per side) with serotype-5 adeno-associated viral vectors (AAV_5) that carried an enhanced third-generation version of the yellow light-sensitive chloride-pump *Natronomonas pharaonis* halorhodopsin (eNpHR3.0), which was fused to the enhanced yellow fluorescent protein (eYFP) and was expressed under the control of the Ca^{2+}/calmodulin-dependent protein kinase II alpha (CaMKIIα) promoter (AAV_5-CaMKIIα-eNpHR3.0-eYFP). For activation, the BLA was transfected unilaterally with similar viruses that coded for the blue light-sensitive cation-pump *Chlamydomonas reinhardtii* channelrhodopsin-2 (ChR2) fused with eYFP (AAV_5-CaMKIIα-ChR2(H134R)-eYFP). Mice in the control groups were transduced with viruses mediating expression of eYFP alone (AAV_5-CaMKIIα-eYFP). All viral aliquots were obtained from the University of North Carolina Vector Core (Chapel Hill, NC). The DNA sequence maps for these viral constructs can be found online at www.optogenetics.org. Following viral infusion, needles were kept at the infusion site for ~10 min to allow for viral diffusion. They were then slowly withdrawn at an approximate rate of ~1 mm/min.

Optical fibers were chronically implanted over the mPFC to either inhibit or activate BLA terminals (optical fiber length, 3 mm; 300-μm core; NA = 0.37; Thorlabs, Newton, NJ). Optical fibers were held in stainless steel ferrules (Precision Fiber Products, Milpitas, CA). The stereotaxic coordinates used for unilateral fiber implants were +1.7 mm AP, ±0.3 mm ML, and −1.9 mm DV, relative to bregma. For bilateral implants, fibers were implanted with a 10° angle and the stereotaxic coordinates used were +1.7 mm AP, ±0.9 mm ML, and −2.1

mm DV. Fiber implants were anchored to the skull with a layer of adhesive cement (C&B Metabond; Parkell, Edgewood, NY) and covered with a layer of black dental cement (Ortho-Jet; Lang, Wheeling, IL). The incision was securely closed using sutures. Postoperative recovery was facilitated by maintaining body temperature using a heat lamp and reducing pain with Ketoprofen (5 mg/kg) or Meloxicam analgesic (1.5 mg/kg). ~5 weeks were allowed for viral expression before behavioral testing.

2.3 Optical manipulations

Optical fibers were connected to patchcords (Doric; Québec, Canada), which were in turn connected to lasers (OEM Laser Systems; Draper, UT) with FC/PC adapters located over the behavioral testing arenas. Laser output was controlled with a Master-8 pulse stimulator (A.M.P.I.; Jerusalem, Israel). For NpHR experiments, a 100-mW 594-nm DPSS laser was used to deliver 5 mW of constant yellow light. For ChR2 experiments, a 100-mW 473-nm DPSS laser was used to deliver 5-ms pulses of blue light at 5 mW and at a frequency of 20 Hz.

2.4 Behavioral assays

All behavioral tests were performed during the active dark phase of the animals. Mice were allowed to acclimate to the testing rooms for at least 1 hr prior to experiments.

2.4.1 Elevated plus maze (EPM)—The EPM apparatus consisted of two open arms (30 × 5 cm) and two enclosed arms (30 × 5 × 30 cm) extending from a central intersection platform (5 × 5 cm). The apparatus was elevated 75 cm from the floor. Mice were connected to the patch cables, placed in the center of the apparatus, and allowed 1–5 min for recovery from handling before behavioral assessment, which lasted 9 min. The test session was divided into 3-min epochs with alternating laser manipulation (OFF-ON-OFF). An EthoVision-XT video tracking system (Noldus; Wageningen, Netherlands) was used to track the mouse location in the apparatus. Mouse location was quantified relative to the body.

2.4.2 Open field test (OFT)—The open field arena consisted of a transparent Plexiglas cube (50 × 50 × 53 cm), and it was divided into a center zone (25 × 25 cm) and an outer zone in the periphery. Mice were connected to the patch cables, placed in the center, and allowed 1–3 min to recover from handling before assessment for 9 min. The OFT session was divided in 3-min epochs with alternating laser manipulation (OFF-ON-OFF). OFT was also assessed with EthoVision-XT video tracking. Mouse location, movement, and velocity were assessed. All measurements were quantified relative to the mouse body.

2.4.3 Social interaction assay—A resident-juvenile-intruder paradigm was used to test social interaction. The test mouse was allowed to freely explore his homecage for 1 min (habituation phase). Then, an unfamiliar juvenile male mouse was introduced for 3 min (test phase). This test was performed twice over two days with different juvenile intruders each day. The amount of time the test mice spent performing social behaviors was scored using commercial software (ODLog™; Macropod Software). The social behaviors quantified include body sniffing, anogenital sniffing, direct contact (e.g., pushing the snout or head underneath the juvenile's body, or crawling over or under the juvenile's body), and close

chasing (within 1-cm distance). These behaviors were summed up to calculate an overall social interaction score for each mouse. Non-social behaviors were also quantified, including digging, walking, rearing, self-grooming, and freezing. Digging, walking, and rearing were summed up to calculate an overall exploration score for each mouse. Each test mouse underwent two social interaction sessions that lasted 3 min and were separated by an interval of 24 hr. Laser manipulation was done in only one of the sessions in a counterbalanced manner across animals.

2.5 Histology

Mice were sacrificed with a lethal dose of sodium pentobarbital (20–30 mg/kg) and then transcardially perfused with ice-cold 4% paraformaldehyde (PFA, pH = 7.3). Brains were extracted, fixed in 4%-PFA overnight, and equilibrated in 30% sucrose. Coronal sections at 40 μm were made using a sliding microtome (HM430; Thermo Fisher Scientific, Waltham, MA).

2.5.1 Immunohistochemistry—Expression of the immediate early gene cfos was measured as a readout of neuronal activity. Induction of cfos was achieved by photostimulating BLA terminals within the mPFC 90 min prior sacrificing the mice (stimulation occurred in the homecage for 3-min). Common immunohistochemistry procedures were used to stain for cfos. Briefly, brain sections were washed in Triton 0.3%/PBS and 3% normal donkey serum for 1 hr, and then incubated in rabbit anti-c-fos primary antibody (1:500 dilution; Calbiochem) for 17–20 hr. Brain sections were washed 4 times in 1X-PBS for 10 min, then incubated in anti-rabbit secondary antibody (AlexaFlour 647, 1:500 dilution; Invitrogen) for 2 hr at room temperature. Four more washes in 1X-PBS were made prior and after a 30-min incubation in a DNA specific fluorescent probe (DAPI: 4′,6-Diamidino-2-Phenylindole; 1:50,000 dilution). Sections were then mounted onto microscope slides with PVD-DABCO mounting media.

2.5.2 Confocal microscopy—Fluorescence images were acquired with an Olympus FV1000 confocal laser scanning microscope, using a 10X/0.40NA, 20X/0.75NA, or a 40X/1.30NA oil immersion objective. Confocal images and serial Z-stacks covering a depth of 10 μm were acquired using an image analysis software (Fluoview; Olympus, Center Valley, PA). Expression of eYFP, cfos, and DAPI was examined in tissue containing various anterior-posterior coronal levels of the BLA and the mPFC. Mice with eYFP expression in cell bodies outside the primary infusion target, the BLA, were excluded from the study.

2.6 Statistics

Two-way analysis of variance (ANOVA) was used with group and laser manipulation as variables (GraphPad Prism Software; La Jolla, CA). Bonferroni-corrected *post-hoc* t-tests were used to detect significant differences. In all statistical tests, the significance threshold was set at $p < 0.05$, and p-values were adjusted to correct for multiple comparisons when appropriate. Error bars indicate mean ± S.E.M.

3.0 Results

3.1 Stimulation of BLA projections to the mPFC produced anxiogenic effects

The BLA was unilaterally transduced with ChR2-eYFP under the control of the CaMKIIα promoter in order to target glutamatergic projection neurons, as previously characterized (Tye et al. 2011). Optical fibers were positioned over the ipsilateral mPFC and 5-ms pulses of blue light at 20 Hz (5 mW) were used to test whether stimulation of BLA inputs to the mPFC could serve to modulate anxiety-like behavior. An eYFP control group was also prepared to control for heating, light artifacts, surgery and tethering. Fig. 1A provides a schematic of the applied optogenetic approach, and Fig. 1B shows representative confocal images of an animal showing expression of ChR2-eYFP in BLA somata and terminals in the mPFC. The location of viral infusion and placement of fibers for each tested animal are shown in sequential coronal drawings in Fig 4.

Anxiety-like behavior was first assessed in the EPM test (ChR2 group n = 9, eYFP group n = 8). Photostimulation of BLA terminals within the mPFC reduced the time mice spent in the open arms (Figs 1C–1D). While two-way ANOVA revealed no significant effect of the group condition ($F_{(1,15)} = 0.30$, $p = 0.59$), it revealed significant effects on laser treatment ($F_{(2,45)} = 7.70$, $p = 0.0013$) and group-by-treatment interaction ($F_{(2,45)} = 3.33$, $p = 0.045$). Bonferroni-corrected post-hoc t-tests showed that ChR2-mice spent significantly less time in the open arms than eYFP-mice during the laser-ON epoch ($p = 0.0008$), and that ChR2-mice spent less time in the open arms during the laser-ON epoch than the preceding laser-OFF epoch ($p = 0.0036$). The probability of entry into the open arms when the animal was in the center of the plus-maze was also significantly lower for ChR2-mice during laser-ON epoch (Fig. 1E; group, $F_{(1,15)} = 5.69$, $p = 0.031$; laser, $F_{(2,30)} = 1.48$, $p = 0.24$; interaction, $F_{(2,30)} = 2.08$, $p = 0.1421$; ChR2 versus eYFP: $p = 0.0012$, Bonferroni corrected for multiple comparisons). These findings indicate that photostimulation of BLA projections in the mPFC is sufficient to increase anxiety-related behavior.

To strengthen the above findings, we also tested anxiety-like behavior in the OFT (ChR2 group n = 9, eYFP group n = 8). Photostimulation of the BLA-mPFC pathway reduced the time mice spent exploring the center of the open-field arena (Figs 1F–1G). A two-way ANOVA revealed significant effects for group condition ($F_{(1,15)} = 6.61$, $p = 0.021$), laser treatment ($F_{(1,15)} = 3.66$, $p = 0.075$), and interaction $F_{(1,15)} = 9.59$, p 0.007). Post-hoc tests confirmed significant differences within the ChR2 group when comparing the laser-ON and laser-OFF epochs ($p = 0.019$), as well as between the ChR2 and eYFP groups during the ON epoch ($p = 0.003$). Activation of the BLA-mPFC pathway did not affect the total distance traveled by mice in the OFT (Fig. 1H; group, $F_{(1,15)} = 0.46$, $p = 0.51$; laser, $F_{(1,15)} = 0.59$, $p = 0.45$; interaction, $F_{(1,15)} = 1.94$, $p = 0.18$). Collectively, these findings indicate that activation of the BLA-mPFC increased anxiety-related behaviors.

3.2 Stimulation of BLA projections to the mPFC reduced social behavior

We next tested whether activation of the BLA-mPFC pathway affects social behavior. We used the resident-juvenile-intruder paradigm in which each “resident” test mouse was presented with an “intruder” juvenile mouse in the homecage, and social and non-social

behaviors were examined. This test was performed twice in two separate days with counterbalanced laser treatment across animals. Different juvenile intruders were used each day. A schematic of the social paradigm and laser manipulations are provided in Fig. 2A.

Stimulation of the BLA-mPFC pathway reduced social interaction (ChR2 group n = 12, eYFP group n = 10). Quantification and summation of close-chasing, body contact, body sniffing, and anogenital sniffing behavior provided an overall social-time score. Fig. 2B shows the average social interaction time. Two-way ANOVA showed significant effects for group condition ($F_{(1,20)} = 8.54$, $p = 0.008$), laser treatment ($F_{(1,20)} = 5.37$, $p = 0.03$), and interaction $F_{(1,15)} = 5.18$, p 0.034). Post-hoc tests corrected for multiple comparisons confirmed that ChR2-mice showed significantly lower overall social interaction scores than eYFP-mice during the laser-ON session ($p = 0.0004$). ChR2-mice also showed reduced social interaction during the ON session relative to the OFF session ($p = 0.0004$).

No significant differences were detected in non-social self-grooming behavior (Fig. 2C; group, $F_{(1,20)} = 0.00$, $p = 0.97$; laser, $F_{(1,20)} = 0.17$, $p = 0.68$; interaction, $F_{(1,20)} = 0.51$, $p = 0.48$). Non-social behaviors related to homecage exploration such as walking, rearing, and digging were also scored. A significant increase in the overall exploration time was induced by photoactivation (Fig. 2D), as a two-way ANOVA showed a significant effect for group condition ($F_{(1,20)} = 8.36$, $p = 0.009$), laser treatment ($F_{(1,20)} = 6.53$, $p = 0.019$) and interaction ($F_{(1,20)} = 7.68$, $p = 0.012$). Post-hoc tests detected a significant difference between the ChR2 and eYFP groups during the laser-ON epoch ($p = 0.0004$, corrected for multiple comparisons). This increase in exploration time could be attributed to the significant decrease in social time. However, no significant differences were observed on freezing/immobilization behavior (Fig. 2E; group, $F_{(1,20)} = 0.03$, $p = 0.87$; laser, $F_{(1,20)} = 0.20$, $p = 0.66$; interaction, $F_{(1,20)} = 0.00$, $p = 0.98$). A summary of the time spent performing each social and non-social behavior is shown in Fig. 2F, and the corresponding means ± SEM can be found in Table 1. Thus, photoactivation of the BLA-mPFC pathway reduced social behavior without altering stereotypical self-grooming behavior or nonspecific freezing responses.

3.3 Stimulation of BLA terminals within the mPFC increased cfos expression in the mPFC, without increasing cfos expression in BLA somata

We quantified expression of the immediate early gene cfos as a readout of neural activity to explore the possibility of confounds produced by activation of BLA somata with our photostimulation procedure of BLA terminals within the mPFC. Activation of BLA somata in this case is possible through either back-propagating action potentials due to antidromic activation of BLA axons or orthodromic activation of BLA somata via descending mPFC projections (Gabbott et al. 2005; Likhtik et al. 2005).

Fig. 3A shows confocal images of the BLA taken at 40X from representative ChR2 and eYFP mice that were photostimulated ~90 min prior to being sacrificed (ChR2 group n = 9, eYFP group n = 8). Fig. 3B shows quantification of eYFP-positive (eYFP+) cells (green) and cfos-positive (cfos+) cells (red) in the BLA, relative to the total number of cells showing DAPI expression. No significant differences were detected between the ChR2 and eYFP-control groups in the proportion of eYFP+ cells ($t_{(15)} = 0.57$, $p = 0.28$), suggesting that any

possible differences in cfos expression could not be attributed to differences in the degree of viral infection. No detectable difference was observed in the proportion of cfos+ BLA cells between ChR2 and eYFP groups (Fig. 3B; $t_{(15)} = 0.39$, $p = 0.39$). While this cannot rule out the possibility of back-propagating action potentials affecting the activity of BLA somata, they are consistent with the idea that the behavioral effects that we observed were produced by activation of BLA projections to the mPFC in the absence of substantial BLA cell body activation.

We also quantified cfos expression in the mPFC to examine whether stimulation of BLA terminals was actually sufficient to trigger mPFC activity. In order to investigate the extent of photoactivation, cfos quantification was done in both mPFC subregions; Prelimbic Cortex (PL) and Infralimbic Cortex (IL). Fig. 3C and Fig. 3E shows confocal images of PL and IL respectively from representative ChR2 and eYFP mice that were sacrificed ~90 min after photostimulation of BLA terminals. Fig. 3D and Fig. 3F shows the quantification of eYFP+ (green) and cfos+ (red) cells within the PL and IL, respectively. As expected, eYFP+ cell bodies within the PL and IL were nearly undetectable in both the ChR2 and eYFP-control groups, as the viruses we used are anterograde and were delivered into the BLA. The ChR2 group however showed significantly higher expression of cfos+ cells in both PL and IL than the eYFP-control group (PL, $t_{(15)} = 3.03$, $p = 0.0042$; IL $t_{(15)}=3.60$, p = 0.0014). This indicates that photostimulation of BLA inputs was sufficient to induce postsynaptic activation of both subregions within the mPFC neurons. We show our histologically verified placements in Figure 4. These results, however, do not rule out the possibility of photostimulation of fibers of passage through the mPFC to elsewhere in the frontal cortex.

3.4 Inhibition of BLA projections to the mPFC produced anxiolytic effects

Although our findings thus far indicate that photoactivation of BLA inputs to the mPFC induces anxiety-like behavior, it remained to be determined whether or not photoinhibition of this pathway reduces anxiety. To examine this possibility, we transduced the BLA bilaterally with NpHR-eYFP or the eYFP control, and optical fibers were bilaterally positioned over the mPFC to allow for photoinhibition with yellow light (Fig. 5A; yellow light was constant at 5 mW). We bilaterally photoinhibited the BLA-mPFC projection to prevent hemispheric compensation. Confocal images in Fig. 5A show BLA somata, and terminals within the mPFC, expressing NpHR-eYFP (NpHR group n = 10, eYFP group n = 9).

Next, we also tested the effect of photoinhibiting the BLA-mPFC projection in the OFT. Fig. 5B shows representative OFT tracks of an NpHR-mouse during a laser-OFF and laser-ON epoch. This representative animal spent more time in the center zone during the ON epoch, indicating a reduction in anxiety. Fig. 5C shows quantification of the average time that NpHR and eYFP mice spent exploring the center zone during the OFF and ON epochs. A two-way ANOVA did not detect significant effects for group condition ($F_{(1,17)} = 2.01$, $p = 0.17$) nor laser treatment alone ($F_{(1,17)} = 3.05$, $p = 0.099$), but detected a significant interaction between the two ($F_{(1,17)} = 5.08$, $p = 0.038$). Post-hoc tests revealed that NpHR-mice spent significantly more time in the center zone than eYFP-mice during the laser-ON epoch ($p = 0.045$, Bonferroni corrected). Interestingly, there was a trend for NpHR-mice to

continue exploring the center zone more than eYFP-mice after the laser was turned OFF (see inset in Fig. 5C; $p = 0.099$, Bonferroni corrected). Photoinhibition of the BLA-mPFC pathway did not alter the total distance that mice traveled in the OFT (Fig. 5D; group, $F_{(1,17)} = 0.09$, $p = 0.77$; treatment, $F_{(1,17)} = 0.00$, $p = 1.00$; interaction, $F_{(1,17)} = 1.85$, $p = 0.19$). These findings indicate that photoinhibition of the BLA-mPFC pathway reduces anxiety-like behavior.

3.5 Inhibition of BLA projections to the mPFC facilitated social interaction

While photoactivation of the BLA-mPFC pathway reduced social behavior, we wanted to explore whether photoinhibiting this pathway facilitates social interaction (NpHR group n = 11, eYFP group n = 12). The NpHR and eYFP groups were submitted to the resident-juvenile-intruder paradigm, as represented in Fig. 5E. Photoinhibition of the BLA-mPFC pathway significantly increased the time that NpHR-mice spent engaging in social behaviors (Fig. 5F). A two-way ANOVA showed a trend towards significance for the group condition ($F_{(1,21)} = 3.49$, $p = 0.076$), no significance for laser treatment ($F_{(1,21)} = 0.77$, $p = 0.39$), and a significant interaction between the two ($F_{(1,21)} = 5.26$, $p = 0.032$). Post-hoc tests confirmed that the mean time spent engaging in social interaction during the light-ON epoch was significantly higher for the NpHR group when compared to the eYFP group ($p = 0.045$, Bonferroni corrected). However, the difference between the light-OFF and light-ON epochs within the NpHR group did not reach statistical significance after correcting for multiple comparisons ($p = 0.13$).

No significant effects were observed in stereotypical self-grooming behavior (Fig. 5G; group, $F_{(1,21)} = 2.02$, $p = 0.17$; laser, $F_{(1,21)} = 0.03$, $p = 0.86$; interaction, $F_{(1,21)} = 0.13$, $p = 0.72$). In addition, while NpHR-mice displayed a slight reduction in homecage exploration time during the laser-ON session, this reduction did not reach significance (Fig. 5H; group, $F_{(1,21)} = 1.24$, $p = 0.28$; laser, $F_{(1,21)} = 0.76$, $p = 0.39$; interaction, $F_{(1,21)} = 6.72$ $p = 0.017$; laser-ON versus laser-OFF: corrected $p = 0.40$; NpHR versus eYFP during the laser-ON session: corrected $p = 0.098$). This slight reduction in homecage exploration time could be attributed to the significant increase in social behavior. No significant differences were detected in freezing behavior (Fig. 5I; group, $F_{(1,21)} = 0.16$ $p = 0.69$; laser, $F_{(1,21)} = 0.06$, $p = 0.81$; interaction, $F_{(1,21)} = 0.74$, $p = 0.40$). Fig. 5J shows a summary of the proportion of all social and non-social behaviors that were measured during this NpHR experiment, and the corresponding means ± SEM can be found in Table 2. Taken together, inhibition of the BLA-mPFC pathway reduces anxiety-related behavior and facilitates social interaction. The location of viral infusion and placement of optical fibers for each animal tested are shown in Fig. 6.

4.0 Discussion

The present results demonstrate a causal role for BLA projections to the mPFC in the modulation of anxiety-related and social behaviors. We found that activating the BLA-mPFC projection increases anxiety-like behavior and reduces social interaction, whereas inhibiting this pathway reduces anxiety-like behavior and increases social behavior. Such bidirectional modulation suggests that the BLA-mPFC pathway is implicated in the regulation of the behavioral manifestations of anxiety and sociability.

The functional role of the mPFC in anxiety-related behaviors has been debated (Shah and Treit 2003). Some studies have reported anxiogenic effects of pharmacological inactivation of the mPFC, for example in the EPM test (Lisboa et al. 2010; de Visser et al. 2011). This suggests that the mPFC generates neural signals that normally dampen anxiety-like behavior. However, other studies have reported anxiolytic effects of mPFC inactivation, for example in the Vogel anxiety test (Resstel, Souza, and Guimarães 2008; Lisboa et al. 2010), suggesting that the mPFC is also capable of producing neural signals that increase anxiety-like behavior. It has been argued that such discrepancy is due to differential roles of the mPFC in different anxiety tasks. An expansion of this notion is that distinct sets of inputs to the mPFC are recruited during different anxiety tasks, and likely each input exerts a specific functional role. Our present findings indicate that BLA inputs to the mPFC exert anxiogenic signals in the EPM and OFT anxiety paradigms.

One caveat in our study is that our optogenetic approach did not discriminate between BLA projections to the PL and IL subregions of the mPFC. Growing evidence indicates opposing functional roles for PL and IL in aversive behaviors, such as conditioned fear (Burgos-Robles, Vidal-Gonzalez, and Quirk 2009; Sierra-Mercado, Padilla-Coreano, and Quirk 2011; Bravo-Rivera et al. 2014; Courtin et al. 2014; Do-Monte et al. 2015), and conditioned active avoidance (Bravo-Rivera et al. 2014; Beck et al. 2014). While PL activity facilitates the expression of conditioned fear and avoidance, IL activity facilitates the extinction and suppression of these behaviors. In addition, it was recently shown that populations of BLA neurons that differentially project to PL and IL respectively encode fear conditioning and fear extinction (Senn et al. 2014). Functional differences between PL and IL have also been observed in stress-evoked autonomic responses (Tavares, Corrêa, and Resstel 2009), goal-directed versus habitual appetitive behavior (Balleine and O'Doherty 2010), as well as for drug-seeking behavior (Peters, Kalivas, and Quirk 2009). Thus, future studies using viral strategies to discretely express opsins in the BLA-PL and BLA-IL pathways could shed light onto possible distinct functional roles of these amygdala-prefrontal pathways in anxiety-related and social behaviors. Nevertheless, PL-IL differences have not been observed in previous studies using pharmacological-mediated inactivation (Resstel, Souza, and Guimarães 2008; van Kerkhof et al. 2013).

Although the present findings are consistent with a functional role of the BLA-mPFC pathway in the modulation of anxiety and social related behaviors, there is the possibility of confounds produced by effects on fibers of passage. Given our approach, it is possible that we also targeted BLA fibers passing through the mPFC but terminating in other regions. For example, the BLA also projects to the anterior cingulate cortex (ACC) and orbitofrontal cortex (OFC), which are adjacent to the mPFC and are suspected to also play roles in anxiety-related and social behaviors (Albrechet-Souza et al. 2009; Achterberg et al. 2015). However, the present finding that our optogenetic ChR2-mediated manipulations produced a significant increase in cfos expression in the mPFC suggests that we reliably triggered postsynaptic activity in the mPFC, and that the behavioral effects we observed were associated, at least in part, by BLA activation of the mPFC. Nevertheless, projection-specific optogenetic strategies or occlusion of the effects we observed by pharmacological inactivation of the mPFC prior to CaMKIIα-ChR2 mediated photostimulation could clarify

this issue. In addition, future *ex vivo* whole-cell patch-clamp recording experiments in the mPFC of mice expressing ChR2 in BLA inputs could further elucidate the local circuit mechanism in the mPFC that contribute to the effects we observed in anxiety and social behaviors (as in Felix-Ortiz et al. 2013).

A noteworthy observation in the present study was that inhibition of BLA projections to the mPFC produced a persistent anxiolytic effect that outlasted the photoinhibition epoch (Fig. 5C, inset). One possible explanation for this effect is that bilateral photoinhibition may have produced an altered experience of the open-field (e.g., perception of the center of the apparatus as a “safe” zone) that resulted in plasticity sufficient to maintain lower anxiety levels beyond the photoinhibition epoch. Another possible explanation is that photoinhibition of the BLA input to the mPFC may have produced downstream changes in neuromodulation that persisted for several minutes beyond the illumination epoch. Further experiments would be necessary to determine which of these represents the underlying mechanism of this persistent anxiolytic effect.

Along with the mPFC, we have recently mapped with optogenetics the functional role of other projections of the BLA on the modulation of anxiety-related and social behaviors (Allsop et al. 2014; Janak and Tye 2015). We have observed anxiolytic effects with activation of BLA projections to the CeA, and anxiogenic effects with inhibition of this pathway (Tye et al. 2011). In that study, BLA-CeA activation produced excitation in the centrolateral (CeL) subdivision of CeA, which in turn produced feed-forward inhibition onto the centromedial (CeM) subdivision, which regulates somatic and autonomic manifestations of anxiety through projections to the bed nucleus of the stria terminalis, hypothalamus and brainstem (LeDoux 2000; deCampo and Fudge 2013).

Another BLA output that we have recently examined is the vHPC. While photoactivation of the BLA-vHPC pathway produced anxiogenic effects, photoinhibition produced anxiolytic effects (Felix-Ortiz et al. 2013). Interestingly, we also observed in our previous study that activation of the BLA-vHPC pathway triggered an increase in cfos expression in the mPFC. Given the strong physiological modulation that vHPC monosynaptic projections exert onto the mPFC (Thierry et al. 2000; Tierney et al. 2004), it is thus possible that vHPC-mPFC interactions also play a strong functional role in the modulation of anxiety-like behaviors (Adhikari, Topiwala, and Gordon 2010). In fact, populations of mPFC neurons that show the strongest task-related firing during EPM testing are strongly coupled to theta oscillations in the vHPC (Adhikari, Topiwala, and Gordon 2011). However, it remains to be elucidated what is the net effect that photoactivation or photoinhibition of the vHPC-mPFC pathway has over anxiety-related behaviors. We have also determined that the BLA-vHPC pathway bidirectionally regulates social behaviors, with BLA-vHPC activation decreasing social interaction and inhibition increasing social interaction (Felix-Ortiz and Tye 2014). Therefore, we have made significant progress using optogenetics in the mapping of BLA-mediated circuit mechanisms underlying the dynamic modulation of anxiety-related and social behaviors.

In conclusion, while anxiety-related and social behaviors play a crucial evolutionary role in adaptation to ever-changing environmental and social conditions, it is reasonable that

essential neural circuits controlling anxiety and social behaviors are redundant and widely distributed across subcortical and cortical areas. Our previous studies illustrated vital roles for BLA projections to CeA and vHPC in the regulation of these adaptive behaviors. To further expand our understanding of how the BLA regulates anxiety and social behaviors, the present study represents the importance of BLA projections to the mPFC in the bidirectional modulation of these behaviors.

Acknowledgments

The authors would like to thank Craig P. Wildes for technical assistance. ACFO was supported by a National Research Service Award Institutional Research Training Grant (5T32GM007484-38), ABR was supported by a NARSAD Young Investigator Award (Brain and Behavior Research Foundation) and an NIMH Research Supplement to Promote Diversity in Health-Related Sciences, and CAL was supported by the Integrative Neuronal Systems Fellowship and the James R. Killian Fellowship. K.M.T. is a New York Stem Cell Foundation - Robertson Investigator, a McKnight Scholar and NIH Director's New Innovator and this work was supported by funding from the JPB Foundation, PIIF, PNDRF, JFDP, Whitehall Foundation, Klingenstein Foundation, NARSAD Young Investigator Award, Alfred P Sloan Foundation, New York Stem Cell Foundation, Whitehead Career Development Chair, and NIH R01-MH102441-01 (NIMH).

References

Achterberg, EJ Marijke; van Kerkhof, Linda WM.; Damsteegt, Ruth; Trezza, Viviana; Vanderschuren, Louk JMJ. Methylphenidate and Atomoxetine Inhibit Social Play Behavior through Prefrontal and Subcortical Limbic Mechanisms in Rats. The Journal of Neuroscience. 2015; 35(1):161–69.10.1523/JNEUROSCI.2945-14.2015 [PubMed: 25568111]

Adhikari, Avishek. Distributed Circuits Underlying Anxiety. Frontiers in Behavioral Neuroscience. 2014; 8:112.10.3389/fnbeh.2014.00112 [PubMed: 24744710]

Adhikari, Avishek; Topiwala, Mihir A.; Gordon, Joshua A. Synchronized Activity between the Ventral Hippocampus and the Medial Prefrontal Cortex during Anxiety. Neuron. 2010; 65(2):257–69.10.1016/j.neuron.2009.12.002 [PubMed: 20152131]

Adhikari, Avishek; Topiwala, Mihir A.; Gordon, Joshua A. Single Units in the Medial Prefrontal Cortex with Anxiety-Related Firing Patterns Are Preferentially Influenced by Ventral Hippocampal Activity. Neuron. 2011; 71(5):898–910.10.1016/j.neuron.2011.07.027 [PubMed: 21903082]

Albrechet-Souza L, Borelli KG, Carvalho MC, Brandão ML. The Anterior Cingulate Cortex Is a Target Structure for the Anxiolytic-like Effects of Benzodiazepines Assessed by Repeated Exposure to the Elevated plus Maze and Fos Immunoreactivity. Neuroscience. 2009; 164(2):387–97.10.1016/j.neuroscience.2009.08.038 [PubMed: 19699782]

Allsop, Stephen A.; Vander Weele, Caitlin M.; Wichmann, Romy; Tye, Kay M. Optogenetic Insights on the Relationship between Anxiety-Related Behaviors and Social Deficits. Frontiers in Behavioral Neuroscience. 2014; 8(July)10.3389/fnbeh.2014.00241

American Psychiatric Association. Diagnostic and Statistical Manual of Mental Disorders. 5. Arlington, VA: 2013.

Balleine, Bernard W.; O'Doherty, John P. Human and Rodent Homologies in Action Control: Corticostriatal Determinants of Goal-Directed and Habitual Action. Neuropsychopharmacology. 2010; 35(1):48–69.10.1038/npp.2009.131 [PubMed: 19776734]

Beck, Kevin D.; Jiao, Xilu; Smith, Ian M.; Myers, Catherine E.; Pang, Kevin CH.; Servatius, Richard J. ITI-Signals and Prelimbic Cortex Facilitate Avoidance Acquisition and Reduce Avoidance Latencies, Respectively, in Male WKY Rats. Frontiers in Behavioral Neuroscience. 2014; 8:403.10.3389/fnbeh.2014.00403 [PubMed: 25484860]

Bickart, Kevin C.; Dickerson, Bradford C.; Barrett, Lisa Feldman. The Amygdala as a Hub in Brain Networks That Support Social Life. Neuropsychologia. 2014; 63(October):235–48.10.1016/j.neuropsychologia.2014.08.013 [PubMed: 25152530]

Bi, Lin-Lin; Wang, Jue; Luo, Zheng-Yi; Chen, Shan-Ping; Geng, Fei; Chen, Yi-hua; Li, Shu-Ji; Yuan, Chun-hua; Lin, Song; Gao, Tian-Ming. Enhanced Excitability in the Infralimbic Cortex Produces

Anxiety-like Behaviors. Neuropharmacology. 2013; 72(September):148–56.10.1016/j.neuropharm.2013.04.048 [PubMed: 23643746]

Boyden, Edward S.; Zhang, Feng; Bamberg, Ernst; Nagel, Georg; Deisseroth, Karl. Millisecond-Timescale, Genetically Targeted Optical Control of Neural Activity. Nature Neuroscience. 2005; 8(9):1263–68.10.1038/nn1525 [PubMed: 16116447]

Bravo-Rivera, Christian; Roman-Ortiz, Ciorana; Brignoni-Perez, Edith; Sotres-Bayon, Francisco; Quirk, Gregory J. Neural Structures Mediating Expression and Extinction of Platform-Mediated Avoidance. The Journal of Neuroscience. 2014; 34(29):9736–42.10.1523/JNEUROSCI.0191-14.2014 [PubMed: 25031411]

Bremner, J Douglas. Brain Imaging in Anxiety Disorders. Expert Review of Neurotherapeutics. 2004; 4(2):275–84.10.1586/14737175.4.2.275 [PubMed: 15853569]

Burgos-Robles, Anthony; Vidal-Gonzalez, Ivan; Quirk, Gregory J. Sustained Conditioned Responses in Prelimbic Prefrontal Neurons Are Correlated with Fear Expression and Extinction Failure. The Journal of Neuroscience. 2009; 29(26):8474–82.10.1523/JNEUROSCI.0378-09.2009 [PubMed: 19571138]

Courtin, Julien; Chaudun, Fabrice; Rozeske, Robert R.; Karalis, Nikolaos; Gonzalez-Campo, Cecilia; Wurtz, Hélène; Abdi, Azzedine; Baufreton, Jerome; Bienvenu, Thomas CM.; Herry, Cyril. Prefrontal Parvalbumin Interneurons Shape Neuronal Activity to Drive Fear Expression. Nature. 2014; 505(7481):92–96.10.1038/nature12755 [PubMed: 24256726]

Davis M. The Role of the Amygdala in Fear and Anxiety. Annual Review of Neuroscience. 1992; 15(1):353–75.10.1146/annurev.ne.15.030192.002033

deCampo, Danielle M.; Fudge, Julie L. Amygdala Projections to the Lateral Bed Nucleus of the Stria Terminalis in the Macaque: Comparison with Ventral Striatal Afferents. The Journal of Comparative Neurology. 2013; 521(14)10.1002/cne.23340

Deisseroth, Karl. Optogenetics. Nature Methods. 2011; 8(1):26–29.10.1038/nmeth.f.324 [PubMed: 21191368]

De Visser, Leonie; Baars, Annemarie; van 't Klooster, Jose; van den Bos, Ruud. Transient Inactivation of the Medial Prefrontal Cortex Affects Both Anxiety and Decision-Making in Male Wistar Rats. Decision Neuroscience. 2011; 5:102.10.3389/fnins.2011.00102

Dias, Brian G.; Banerjee, Sunayana B.; Goodman, Jared V.; Ressler, Kerry J. Towards New Approaches to Disorders of Fear and Anxiety. Current Opinion in Neurobiology. 2013; 23(3):346–52.10.1016/j.conb.2013.01.013 [PubMed: 23402950]

Do-Monte, Fabricio H.; Manzano-Nieves, Gabriela; Quiñones-Laracuente, Kelvin; Ramos-Medina, Liorimar; Quirk, Gregory J. Revisiting the Role of Infralimbic Cortex in Fear Extinction with Optogenetics. The Journal of Neuroscience. 2015; 35(8):3607–15.10.1523/JNEUROSCI.3137-14.2015 [PubMed: 25716859]

Felix-Ortiz, Ada C.; Beyeler, Anna; Seo, Changwoo; Leppla, Christopher A.; Wildes, Craig P.; Tye, Kay M. BLA to vHPC Inputs Modulate Anxiety-Related Behaviors. Neuron. 2013; 79(4):658–64.10.1016/j.neuron.2013.06.016 [PubMed: 23972595]

Felix-Ortiz, Ada C.; Tye, Kay M. Amygdala Inputs to the Ventral Hippocampus Bidirectionally Modulate Social Behavior. The Journal of Neuroscience. 2014; 34(2):586–95.10.1523/JNEUROSCI.4257-13.2014 [PubMed: 24403157]

Freitas-Ferrari, Maria Cecilia; Hallak, Jaime EC.; Trzesniak, Clarissa; Filho, Alaor Santos; Machado-de-Sousa, João Paulo; Chagas, Marcos Hortes N.; Nardi, Antonio E.; Crippa, José Alexandre S. Neuroimaging in Social Anxiety Disorder: A Systematic Review of the Literature. Progress in Neuro-Psychopharmacology and Biological Psychiatry. 2010; 34(4):565–80.10.1016/j.pnpbp.2010.02.028 [PubMed: 20206659]

Gabbott, Paul LA.; Warner, Tracy A.; Jays, Paul RL.; Salway, Phillip; Busby, Sarah J. Prefrontal Cortex in the Rat: Projections to Subcortical Autonomic, Motor, and Limbic Centers. The Journal of Comparative Neurology. 2005; 492(2):145–77.10.1002/cne.20738 [PubMed: 16196030]

Gotts, Stephen J.; Kyle Simmons, W.; Milbury, Lydia A.; Wallace, Gregory L.; Cox, Robert W.; Martin, Alex. Fractionation of Social Brain Circuits in Autism Spectrum Disorders. Brain. 2012; 135(9):2711–25.10.1093/brain/aws160 [PubMed: 22791801]

Hoover, Walter B.; Vertes, Robert P. Anatomical Analysis of Afferent Projections to the Medial Prefrontal Cortex in the Rat. Brain Structure and Function. 2007; 212(2):149–79.10.1007/s00429-007-0150-4 [PubMed: 17717690]

Janak, Patricia H.; Tye, Kay M. From Circuits to Behaviour in the Amygdala. Nature. 2015; 517(7534):284–92.10.1038/nature14188 [PubMed: 25592533]

Jodo E, Katayama T, Okamoto M, Suzuki Y, Hoshino K, Kayama Y. Differences in Responsiveness of Mediodorsal Thalamic and Medial Prefrontal Cortical Neurons to Social Interaction and Systemically Administered Phencyclidine in Rats. Neuroscience. 2010; 170(4):1153–64.10.1016/j.neuroscience.2010.08.017 [PubMed: 20727386]

Katayama T, Jodo E, Suzuki Y, Hoshino K-Y, Takeuchi S, Kayama Y. Phencyclidine Affects Firing Activity of Basolateral Amygdala Neurons Related to Social Behavior in Rats. Neuroscience. 2009; 159(1):335–43.10.1016/j.neuroscience.2009.01.002 [PubMed: 19162135]

Kennedy, Daniel P.; Adolphs, Ralph. The Social Brain in Psychiatric and Neurological Disorders. Trends in Cognitive Sciences. 2012; 16(11):559–72.10.1016/j.tics.2012.09.006 [PubMed: 23047070]

Kling A, Steklis HD. A Neural Substrate for Affiliative Behavior in Nonhuman Primates. Brain, Behavior and Evolution. 1976; 13(2–3):216–38.10.1159/000123811

LeDoux, Joseph E. Emotion Circuits in the Brain. Annual Review of Neuroscience. 2000; 23(1):155–84.10.1146/annurev.neuro.23.1.155

Likhtik, Ekaterina; Paz, Rony. Amygdala–prefrontal Interactions in (mal)adaptive Learning. Trends in Neurosciences. 201510.1016/j.tins.2014.12.007

Likhtik, Ekaterina; Pelletier, Joe Guillaume; Paz, Rony; Paré, Denis. Prefrontal Control of the Amygdala. The Journal of Neuroscience. 2005; 25(32):7429–37.10.1523/JNEUROSCI.2314-05.2005 [PubMed: 16093394]

Likhtik, Ekaterina; Stujenske, Joseph M.; Topiwala, Mihir A.; Harris, Alexander Z.; Gordon, Joshua A. Prefrontal Entrainment of Amygdala Activity Signals Safety in Learned Fear and Innate Anxiety. Nature Neuroscience. 2014; 17(1):106–13.10.1038/nn.3582 [PubMed: 24241397]

Lisboa SF, Stecchini MF, Corrêa FMA, Guimarães FS, Resstel LBM. Different Role of the Ventral Medial Prefrontal Cortex on Modulation of Innate and Associative Learned Fear. Neuroscience. 2010; 171(3):760–68.10.1016/j.neuroscience.2010.09.048 [PubMed: 20883749]

McClure, Erin B.; Monk, Christopher S.; Nelson, Eric E.; Parrish, Jessica M.; Adler, Abby; James, R.; Blair, R.; Fromm, Stephen, et al. Abnormal Attention Modulation of Fear Circuit Function in Pediatric Generalized Anxiety Disorder. Archives of General Psychiatry. 2007; 64(1):97–106.10.1001/archpsyc.64.1.97 [PubMed: 17199059]

Milad, Mohammed R.; Rauch, Scott L. The Role of the Orbitofrontal Cortex in Anxiety Disorders. Annals of the New York Academy of Sciences. 2007; 1121(1):546–61.10.1196/annals.1401.006 [PubMed: 17698998]

Peters, Jamie; Kalivas, Peter W.; Quirk, Gregory J. Extinction Circuits for Fear and Addiction Overlap in Prefrontal Cortex. Learning & Memory. 2009; 16(5):279–88.10.1101/lm.1041309 [PubMed: 19380710]

Pitkänen A. Connectivity of the Rat Amygdaloid Complex. The Amygdala: A Functional Analysis. 2000; 2:31–115.

Rauch, Scott L.; Shin, Lisa M.; Wright, Christopher I. Neuroimaging Studies of Amygdala Function in Anxiety Disorders. Annals of the New York Academy of Sciences. 2003; 985(1):389–410.10.1111/j.1749-6632.2003.tb07096.x [PubMed: 12724173]

Resstel LBM, Souza RF, Guimarães FS. Anxiolytic-like Effects Induced by Medial Prefrontal Cortex Inhibition in Rats Submitted to the Vogel Conflict Test. Physiology & Behavior. 2008; 93(1–2):200–205.10.1016/j.physbeh.2007.08.009 [PubMed: 17884112]

Roozendaal, Benno; McEwen, Bruce S.; Chattarji, Sumantra. Stress, Memory and the Amygdala. Nature Reviews Neuroscience. 2009; 10(6):423–33.10.1038/nrn2651 [PubMed: 19469026]

Rosenkranz, J Amiel; Venheim, Emily R.; Padival, Mallika. Chronic Stress Causes Amygdala Hyperexcitability in Rodents. Biological Psychiatry, Amygdala Activity and Anxiety: Stress Effects. 2010; 67(12):1128–36.10.1016/j.biopsych.2010.02.008

Senn, Verena; Wolff, Steffen BE.; Herry, Cyril; Grenier, François; Ehrlich, Ingrid; Gründemann, Jan; Fadok, Jonathan P.; Müller, Christian; Letzkus, Johannes J.; Lüthi, Andreas. Long-Range Connectivity Defines Behavioral Specificity of Amygdala Neurons. Neuron. 2014; 81(2):428–37.10.1016/j.neuron.2013.11.006 [PubMed: 24462103]

Shah, Akeel A.; Treit, Dallas. Excitotoxic Lesions of the Medial Prefrontal Cortex Attenuate Fear Responses in the Elevated-plus Maze, Social Interaction and Shock Probe Burying Tests. Brain Research. 2003; 969(1–2):183–94.10.1016/S0006-8993(03)02299-6 [PubMed: 12676379]

Sierra-Mercado, Demetrio; Padilla-Coreano, Nancy; Quirk, Gregory J. Dissociable Roles of Prelimbic and Infralimbic Cortices, Ventral Hippocampus, and Basolateral Amygdala in the Expression and Extinction of Conditioned Fear. Neuropsychopharmacology: Official Publication of the American College of Neuropsychopharmacology. 2011; 36(2):529–38.10.1038/npp.2010.184 [PubMed: 20962768]

Stein, Murray B.; Stein, Dan J. Social Anxiety Disorder. The Lancet. 2008; 371(9618):1115–25.10.1016/S0140-6736(08)60488-2

Tavares RF, Corrêa FMA, Resstel LBM. Opposite Role of Infralimbic and Prelimbic Cortex in the Tachycardiac Response Evoked by Acute Restraint Stress in Rats. Journal of Neuroscience Research. 2009; 87(11):2601–7.10.1002/jnr.22070 [PubMed: 19326445]

Thierry, Anne-Marie; Gioanni, Yves; Dégénétais, Eric; Glowinski, Jacques. Hippocampo-Prefrontal Cortex Pathway: Anatomical and Electrophysiological Characteristics. Hippocampus. 2000; 10(4): 411–19.10.1002/1098-1063(2000)10:4<411::AID-HIPO7>3.0.CO;2-A [PubMed: 10985280]

Tierney, Patrick L.; Dégenètais, Eric; Thierry, Anne-Marie; Glowinski, Jacques; Gioanni, Yves. Influence of the Hippocampus on Interneurons of the Rat Prefrontal Cortex. European Journal of Neuroscience. 2004; 20(2):514–24.10.1111/j.1460-9568.2004.03501.x [PubMed: 15233760]

Tye, Kay M.; Deisseroth, Karl. Optogenetic Investigation of Neural Circuits Underlying Brain Disease in Animal Models. Nature Reviews. Neuroscience. 2012; 13(4):251–66.10.1038/nrn3171 [PubMed: 22430017]

Tye, Kay M.; Prakash, Rohit; Kim, Sung-Yon; Fenno, Lief E.; Grosenick, Logan; Zarabi, Hosniya; Thompson, Kimberly R.; Gradinaru, Viviana; Ramakrishnan, Charu; Deisseroth, Karl. Amygdala Circuitry Mediating Reversible and Bidirectional Control of Anxiety. Nature. 2011; 471(7338): 358–62.10.1038/nature09820 [PubMed: 21389985]

Van Kerkhof, Linda WM.; Damsteegt, Ruth; Trezza, Viviana; Voorn, Pieter; Vanderschuren, Louk JMJ. Social Play Behavior in Adolescent Rats Is Mediated by Functional Activity in Medial Prefrontal Cortex and Striatum. Neuropsychopharmacology. 2013; 38(10):1899–1909.10.1038/npp.2013.83 [PubMed: 23568326]

Highlights

- BLA projections to the mPFC were targeted using optogenetic tools in mice.
- Stimulation increased anxiety-like behavior and decreased social interaction.
- Inhibition decreased anxiety-like behavior and increased social interaction.

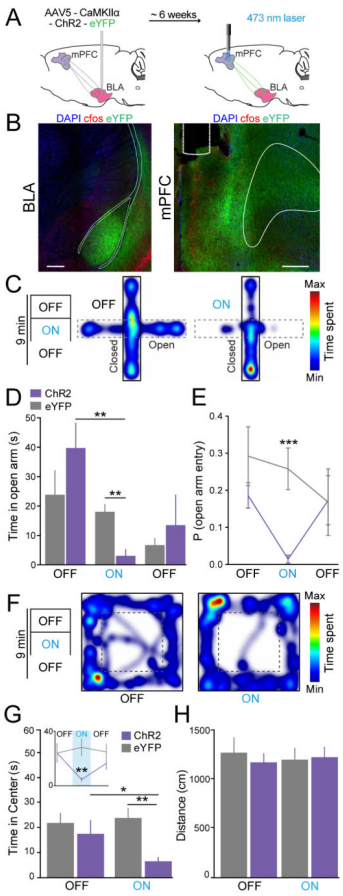

Fig. 1.

Photostimulation of BLA terminals in the mPFC increased anxiety-like behavior. (A) Illustration of infusion of viral vectors allowing expression of either ChR2-eYFP or eYFP alone into the BLA and optical fiber placement over the mPFC for photostimulation (ChR2 group n = 9, eYFP group n = 8). (B) Coronal confocal images (at 20X) show expression of ChR2-eYFP in BLA somata, as well as in BLA terminals within the prelimbic (PL) and infralimbic (IL) subregions of the mPFC (*blue*, DAPI; *red*, cfos; *green*, ChR2-eYFP). (C) Elevated-plus maze (EPM) testing consisted of 3-min epochs with alternating laser manipulation (OFF-ON-OFF). Heat maps show time spent at each location within the maze or chamber for a representative ChR2-mouse during the initial OFF epoch and the ON epoch (*cooler shades represent less time and warmer shades represent more time spent at that location*). (D) ChR2-mice spent significantly less time in the open arms of the EPM during the ON epoch, relative to eYFP-mice and relative to the ChR2 group during the OFF epoch. (E) Photostimulation also reduced the probability to enter the open arms of the EPM. (F) The open-field test (OFT) also consisted of 3-min epochs with alternating laser treatment (OFF-ON-OFF). Heat maps representing the time spent at each location are shown for a ChR2-mouse during the first OFF epoch and the ON epoch. (G) Average time mice spent exploring the center of the OFT arena. The two OFF epochs are combined on the main bar graph, and illustrated individually in the line plot inset. ChR2-mice spent significantly less time in the center of the arena during the ON epoch, relative to eYFP-mice and the OFF

epochs. (H) No significant effects were detected in the total distance travelled by mice in the OFT. In all figures, data are illustrated as mean ± SEM. Numbers within bars indicate the *n*'s per group. ***$p < 0.001$, **$p < 0.01$, *$p < 0.05$, corrected for multiple comparisons.

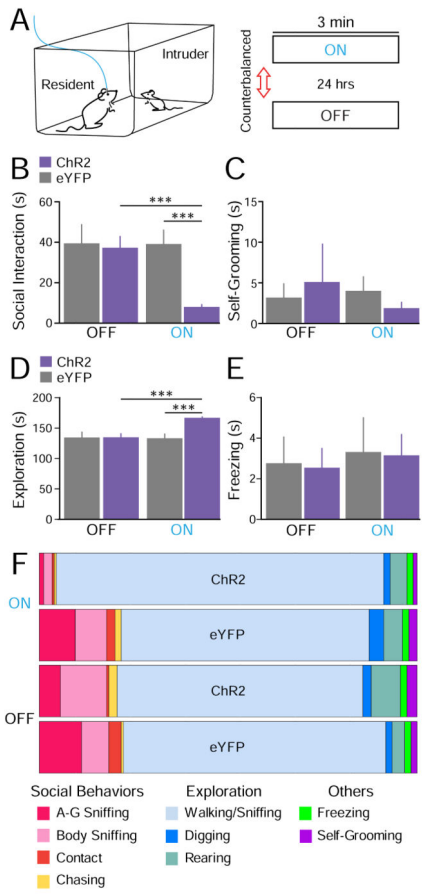

Fig. 2.

Photostimulation of BLA terminals in the mPFC reduced social interaction. (A) Illustration of the resident-juvenile-intruder paradigm. Two 3-min sessions separated by a 24-hr interval were conducted with counterbalanced laser treatment (ChR2 group n = 12, eYFP group n = 10). (B) Average time resident mice spent engaged in social-related behaviors. ChR2-mice spent significantly less time socializing with the juvenile intruders during the laser-ON session than eYFP-mice. (C) No significant differences were detected in self-grooming behavior. (D) A small but significant increase was observed in homecage exploration. (E) No significant differences were observed in freezing/immobilization behavior. (F) Distribution of specific social and non-social behaviors for the entire 3 min epoch (s).

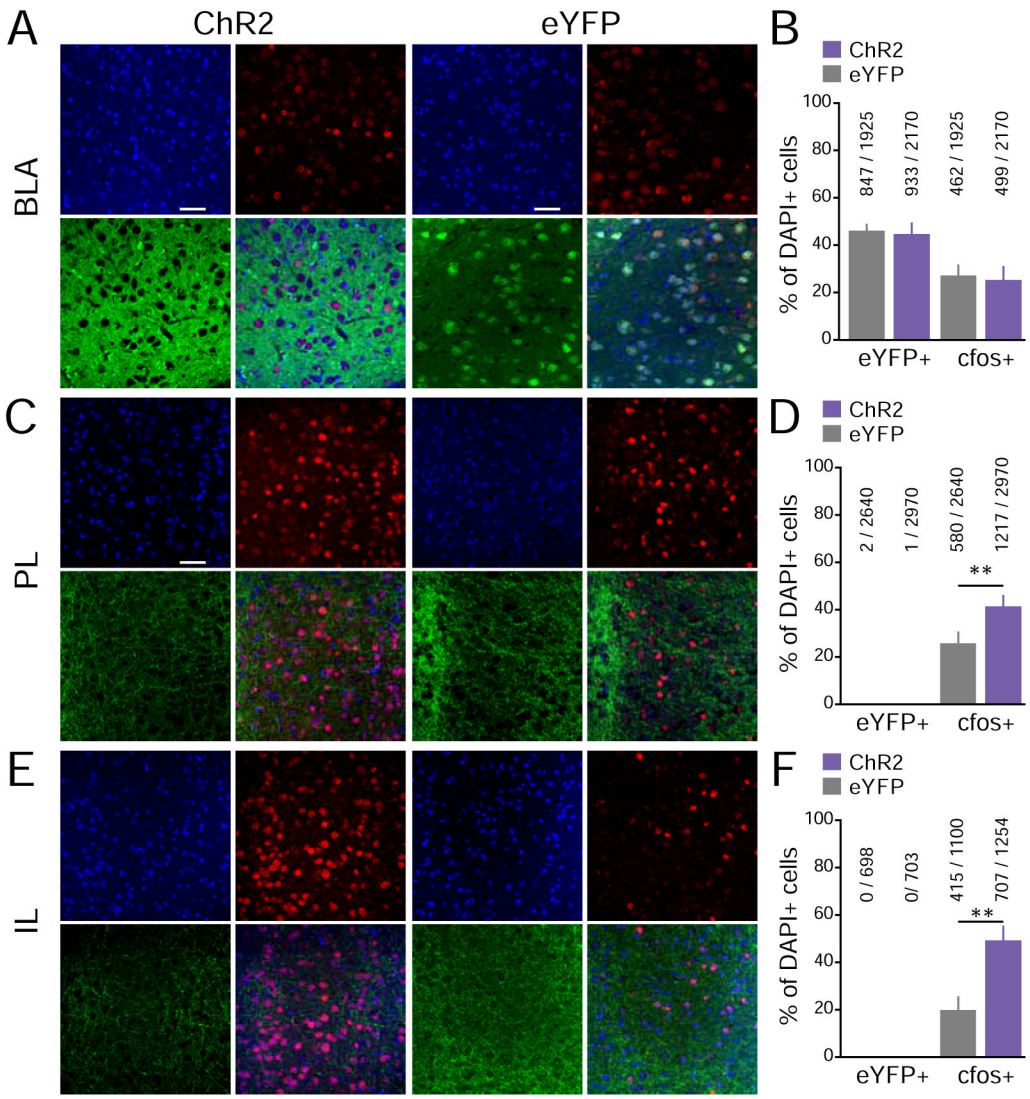

Fig. 3.

Activation of BLA inputs was sufficient to activate mPFC neurons. Mice underwent a 3-min photostimulation session in their homecage ~90 min prior to being sacrificed. Immunoreactivity to cfos was used as a proxy for neuronal activity. (ChR2 group n = 9, eYFP group n = 8). (A) 40X confocal images of the BLA from representative ChR2 and eYFP mice (*blue*: DAPI+ cells, *green*: eYFP+ cells, *red*: cfos+ cells). (B) Percentage of eYFP+ and cfos+ cells in the BLA, relative to the total DAPI+ cell counts. No significant differences were detected between the ChR2 and eYFP-control groups. (C) 40X images of PL sub-regions of the mPFC. (D) Percentage of eYFP+ and cfos+ cells in the PL sub-region of the mPFC, relative to DAPI counts. (E) 40X images of IL sub-regions of the mPFC. (D) Percentage of eYFP+ and cfos+ cells in the IL subr-region of the mPFC, relative to DAPI counts. As expected, almost no mPFC cell was eYFP+. The proportion of cfos+ mPFC (Both PL and IL) cells was significantly higher in the ChR2 group than the eYFP-control group, suggesting that photostimulation of BLA inputs facilitate mPFC activity.

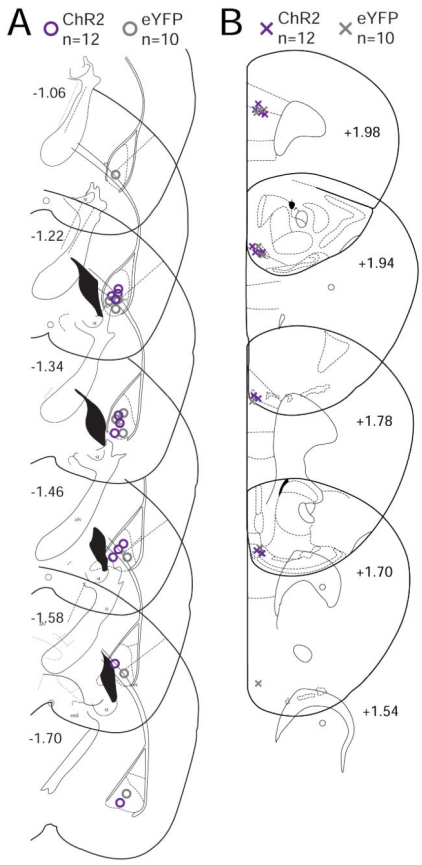

Fig. 4.

Location of viral infusion in the BLA and optical fiber placement in the mPFC for the ChR2 experiments. (A) Coronal drawings across multiple levels of the BLA, relative to bregma, show the center point of viral infusion for each animal (ChR2-mice: *purple circles*, eYFP-mice: *grey circles*). (B) Optical fiber tip in the mPFC for each animal (ChR2-mice: *purple crosses*, eYFP-mice: *grey crosses*).

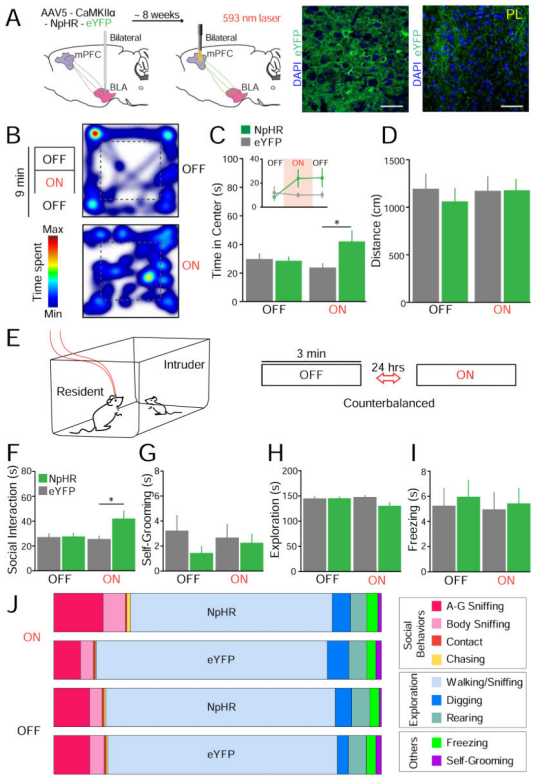

Fig. 5.

Photoinhibition of BLA terminals in the mPFC reduced anxiety-like behavior and facilitated social interaction. (A) Brain schematics illustrate the bilateral photoinhibition approach. Representative confocal images (at 40X) are shown for a mouse in the NpHR group (*blue*: DAPI, *green*: NpHR-eYFP). (B) Heat maps representing time spent at each location in the OFT for an NpHR-mouse during the initial laser-OFF epoch and the laser-ON epoch (NpHR group n = 10, eYFP group n = 9). (C) Mean time in the center zone of the OFT. The two laser-OFF epochs are combined on the main bar graph and illustrated individually in the inset. NpHR-mice spent significantly higher time in the center zone during the laser-ON epoch, relative to eYFP-mice and to the laser-OFF epoch. (D) No significant differences were observed in the total distance travelled by mice in the OFT. (E) Experimental design for the social task (NpHR group n = 11, eYFP group n = 12). (F) NpHR-mice spent significantly more time engaged in social interaction during photoinhibition, relative to eYFP-mice. (G–I) No significant differences were observed on self-grooming (*G*), homecage exploration (*H*), or freezing behavior (*I*). (J) Distribution of specific social and non-social behaviors for the entire epoch.

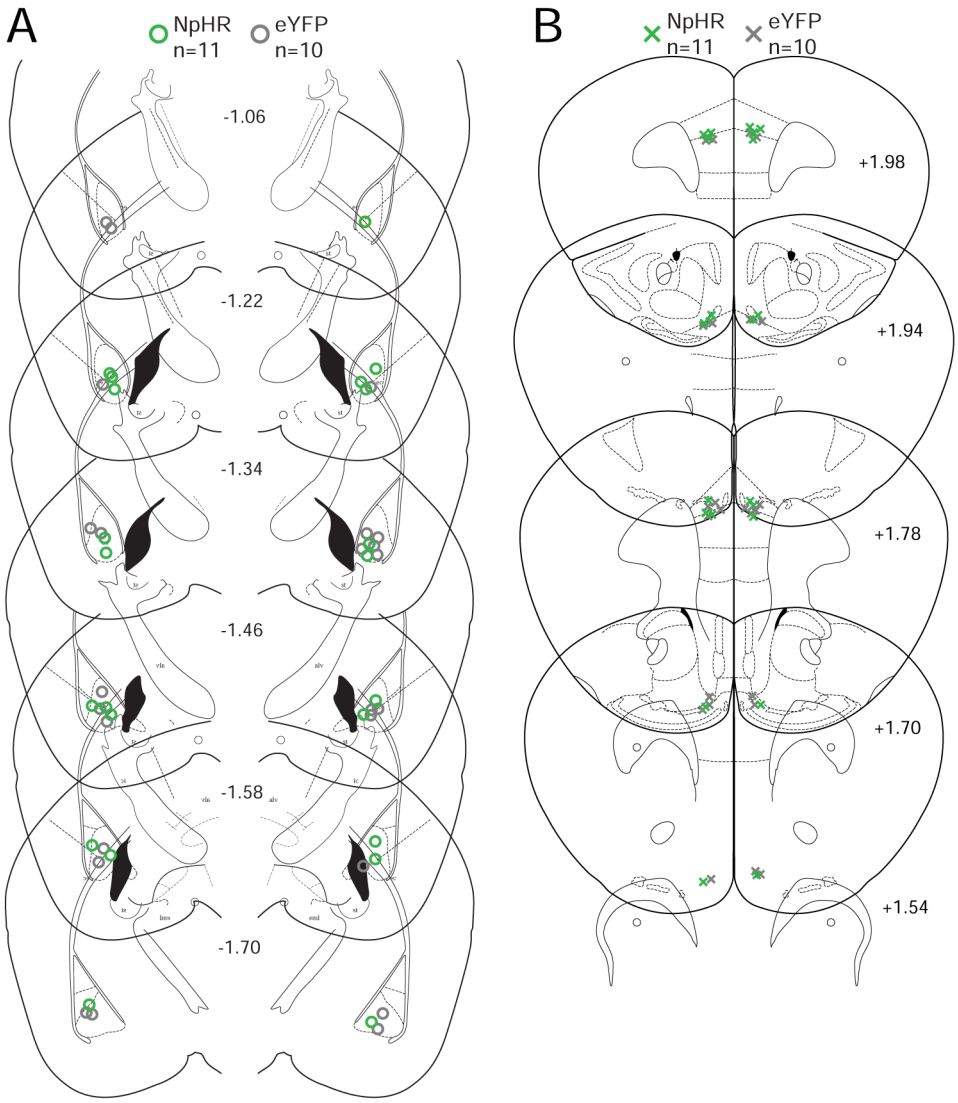

Fig. 6.

Location of viral infusion in the BLA and optical fiber placement in the mPFC for the NpHR experiments. (A) Center point of viral infusion in the bilateral BLA (NpHR-mice: *green circles*, eYFP-mice: *grey circles*). (B) Optical fiber tip in the bilateral mPFC (NpHR-mice: *green crosses*, eYFP-mice: *grey crosses*).

Table 1

Distribution for each behavioral subcategory during activation of BLA – mPFC projecting neurons corresponding to Fig. 2F. Means and ± SEMs for time spent (s) for each of the subcategories quantified for our summed social behavior score (A-G Sniffing, Body Sniffing and Contact) and exploratory behavior score (Walking/Cage Sniffing, Digging, and Rearing). In addition, means and ± SEMs for time spent (s) Freezing and Self-Grooming are also shown. Each columns represent either opsin expressing (ChR2 n = 12) or fluorophore only (eYFP n=10) groups, during either ON or OFF epochs. Each row represents each behavioral sub-category.

	ON		**ON**					
	Mean	**±SEM**	**Mean**	**±SEM**	**Mean**	**±SEM**	**Mean**	**±SEM**
A-G Sniffing	2.39	0.67	17.15	4.71	10.44	3.32	19.6	5.77
Body Sniffing	3.54	0.74	14.78	4.13	21.97	4.69	13.22	3.57
Contact	1.49	0.47	4.35	0.99	1.15	0.26	5.71	2.36
Chasing	0.65	0.29	3.11	1.18	3.79	1.45	0.96	0.48
Walking/Cage sniffing	156.29	2.02	117.44	7.74	116.71	7.17	125.36	8.36
Digging	3.06	0.29	6.63	1.34	4.55	1.00	3.54	1.47
Rearing	7.53	1.36	9.2	2.91	13.73	2.81	5.66	1.85
Freezing	3.16	1.06	3.32	1.77	2.55	0.98	2.77	1.35
Self-Grooming	1.89	0.73	4.02	1.81	5.11	4.86	3.18	1.78

Table 2

Distribution for each behavioral subcategory during inhibition of BLA – mPFC projecting neurons corresponding to Fig. 5J. Means and ± SEMs for time spent (s) for each of the subcategories used for our summed social behavior score (A-G Sniffing, Body Sniffing and Contact) and exploratory behavior score (Walking/Cage Sniffing, Digging, and Rearing). In addition, means and ± SEMs for time spent (s) Freezing and Self-Grooming are also shown. Each columns represent either opsin expressing (NpHR n = 11) or fluorophore only (eYFP n=12) groups, during either ON or OFF epochs. Each row represents each behavioral subcategory.

	ON		**ON**					
	Mean	**±SEM**	**Mean**	**±SEM**	**Mean**	**±SEM**	**Mean**	**±SEM**
A-G Sniffing	26.88	4.87	15.69	2.46	20.16	2.99	20.14	3.20
Body Sniffing	13.26	2.99	6.71	1.32	7.21	1.42	8.06	1.71
Contact	0.41	0.10	0.91	0.20	0.63	0.21	0.48	0.24
Chasing	1.53	1.12	0.29	0.27	0.55	0.31	0.98	0.41
Walking/Cage Sniffing	110.81	7.02	127.65	5.11	126.18	5.17	126.20	5.08
Digging	10.69	4.39	11.72	6.18	8.74	4.31	6.02	2.23
Rearing	8.75	2.34	9.50	2.17	9.61	2.43	9.97	1.95
Freezing	5.85	1.38	4.74	1.33	5.59	1.59	5.21	1.34
Self-Grooming	1.81	0.78	2.79	1.033	1.33	0.59	2.95	1.19